RESEARCH ARTICLE

Same, but different: Variations in fragment ions among stereoisomers of a 17α-methyl steroid in gas chromatography/electron ionization mass spectrometry

Jakob Steff [ORCID] | Maria K. Parr [ORCID]

Institute of Pharmacy, Berlin, Germany

Correspondence
Maria Kristina Parr, Institute of Pharmacy, Freie Universität Berlin, Königin-Luise-Straße 2+4, 14195 Berlin, Germany.
Email: maria.parr@fu-berlin.de

Rationale: Gas chromatography/electron ionization mass spectrometry (GC/EI-MS) is a well-established tool for the identification of unknown compounds such as new metabolites of xenobiotics. But it reaches the limits of confident structural assignment if it comes to stereoisomers. This work helps to overcome this difficulty by getting a deeper comprehension of composition of so far unspecific and also characteristic fragment ions in general and comparison among stereoisomers.

Methods: Unit mass resolution mass spectra of various isotopologues of four 17α-methyl steroid diastereomers obtained by selectively introducing $[^2H_9]$-trimethylsilyl (TMS) groups or chemical syntheses were systematically compared. The impact of stereochemistry on variations of relative abundances has been assessed by statistical comparison from repeated measurements. Additionally, characterization of m/z 318 with high-resolution MS using gas chromatography/quadrupole time-of-flight MS (GC/QTOF-MS) was performed.

Results: The formation of fragment ions from TMS-derivatives after cleavage of methyl or TMS groups ($[M-CH_3]^+$, $[M-TMSOH]^{\bullet+}$, $[M-CH_3-TMSOH]^+$, $[M-2x90]^{\bullet+}$, $[M-2x90-CH_3]^+$) rarely arises from only one position in the molecule and composition of fragment ion signals is highly influenced by the stereochemistry of the A-ring at C3 and C5 of the steroid. Similarly, the formation of the characteristic fragment ion m/z 143 most likely consists of two different ways of formation. A possible structure for fragment ion m/z 318 was postulated.

Conclusions: Stereoisomers showed differing fragmentation behaviors based on their configuration. These observations further illustrate that variations among stereoisomers in EI-MS fragmentation is no random underlying process but instead a pattern which needs to be understood in its complexity. This easily accessible technical approach can be applied on different molecule structures to further investigate the field of isomeric assignment in GC/EI-MS.

1 | INTRODUCTION

One great benefit of working with EI-MS is its high reproducibility of mass spectra irrespective of instrumental setups. This is taken advantage of by identification of compounds without reference material but using mass spectral reference libraries.[1] Regardless of the growing number of databases and algorithms the problem of properly assigning stereoisomers still seems to be challenging.[1–3] This can be explained by the qualitatively identical mass spectra among stereoisomers, which only differ in relative intensities of observed fragment ions.[4]

This challenge can be observed in different disciplines in the analytical community such as of food safety, forensics, and doping of animals or humans. One example is the testing of the administration of anabolic androgenic steroids (AAS) in sport. They are included in the list of prohibited substances and methods published by the World Anti-Doping Agency (WADA) and recently published numbers show that the vast majority of adverse analytical findings belonged to the group of AAS.[5–8] For detection of the misuse techniques of choice are based on chromatographic separation and mass spectrometric detection, mainly GC/EI-MS.[9,10]

Analysis of mass spectrometric fragmentation has been an extensively investigated field for decades. Thevis and Schänzer gave a detailed review especially focusing on the field of sports drug testing.[11] There are two modalities which need to be differentiated discussing fragmentation of AAS in EI-MS, i.e. derivatized or underivatized samples. The most common approach for AAS today is introducing trimethylsilyl (TMS) ethers to hydroxy and carbonyl groups present in the molecules via trimethylsilyl iodide (TMIS), generally generated in situ.[12–15] This alteration highly impacts chemical properties of analytes and leads to an increase of volatility and thermal stability besides altered fragmentation patterns.[16–18] To increase confidence in assignment of fragment ions, stable isotopic labelling depicts a well-established concept.[11,19,20] This might be achieved by introducing deuterium and oxygen-18 by chemical synthesis or simply by introducing labelled [²H₉]-TMS groups from the labelled derivatizing agent.[12,21–25]

The presented work is focusing on fragmentation of the well-known 17ξ-methyl-5ξ-androstane-3ξ,17ξ-diol structure also known as tetrahydromethyltestosterone (THMT) as model substance. THMT can be detected as metabolite after intake of, inter alia, methyltestosterone, metandienone, methandriol and mestanolone.[26] This 17-methyl steroid bears in general stereogenic centers in position C3, C5, C8, C9, C10, C13, C14 and C17, yet only stereoisomers of THMT with inverted C3, C5 and C17 have been detected and seem to be of relevance in anti-doping analysis.[27] In our investigation we concentrated on the four possible 17α-methyl isomers with alternating A-ring stereochemistry to keep a comprehensive scope (Figure 1). Stable isotopic labelling was used to take a closer look at allegedly similar mass spectra and the origin of characteristic fragment ions. Core investigation focused on presumably unspecific fragments corresponding to a loss of methyl groups and TMS groups ([M-CH₃]⁺, [M-TMSOH]•⁺, [M-2x90]•⁺, [M-2x90-CH₃]⁺). By comparison of
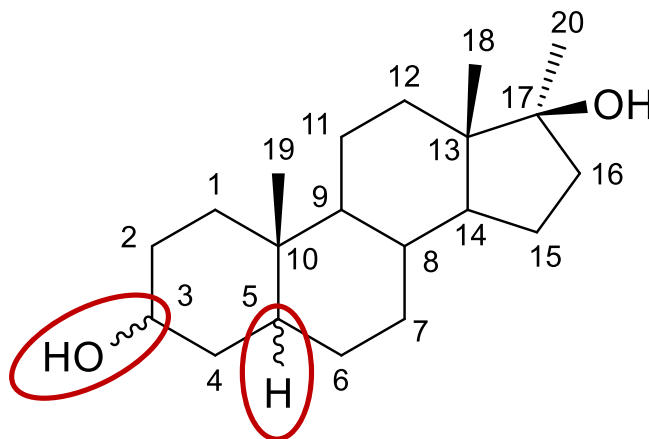

FIGURE 1 Chemical structure and numbering of the carbon backbone of THMT. Stereocenters of interest at C3 and C5 to yield **1.0**, **2.0**, **3.0**, and **4.0** are indicated by wavy bonds and highlighted with red markings. [Color figure can be viewed at wileyonlinelibrary.com]

relative abundances of corresponding signals based on resulting mass shifts e.g. [M-CH₃]⁺ and [M-CD₃]⁺, statements are made about the structural origin of detected ions and contextualized with different behavior of stereoisomers. These investigations were highly inspired by previous work by Kollmeier et al. considering mass spectral fragmentation analyses of isotopically labelled androstanediols.[22] Additionally, repeated measurements of mass spectra were used for comparison of relative abundances of studied fragment ions between four isomers of THMT. The goal was to determine the influence of stereochemistry on fragmentational behavior and the shift of intensities of corresponding signals between these isomers. Following, data nicely illustrates that questioning even supposedly simple things may reveal unexpected complexity.
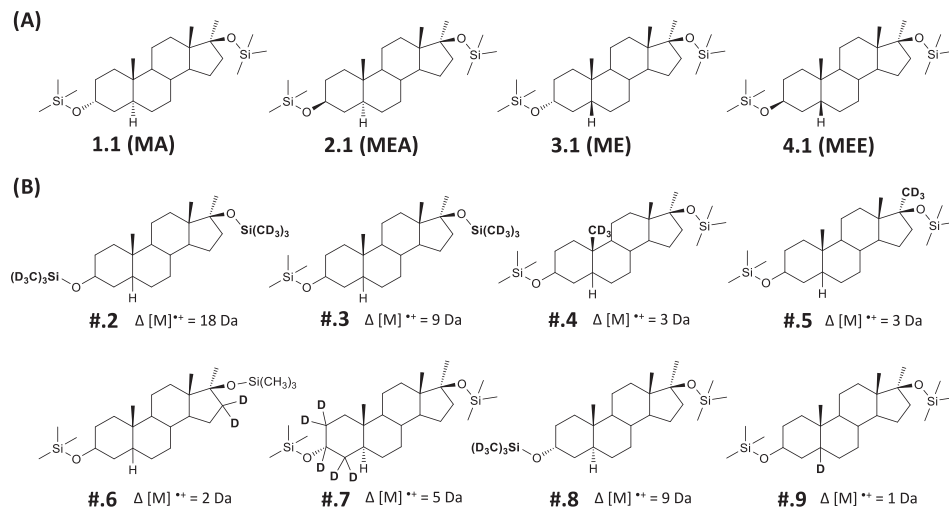
2 | EXPERIMENTAL

2.1 | Reagents and chemicals

Ammonium iodide (≥99%) and ethanethiol (97%) were purchased from Sigma-Aldrich GmbH (Taufkirchen, Germany). N-Methyl-N-(trimethylsilyl)trifluoroacetamide (MSTFA) was purchased from Chemische Fabrik Karl Bucher GmbH (Waldstetten, Germany) and N,O-bis(trimethyl-[²H₉]-silyl)acetamide ([²H₁₈]-BSA) from Abcr GmbH (Karlsruhe, Germany). The following molecule structures were synthesized in house and their chemical structures of their bis-TMS derivatives are schematically displayed in Figure 2: 17α-methyl-5α-androstane-3α,17β-diol (**1.0**), 17α-methyl-5α-androstane-3β,17β-diol (**2.0**), 17α-methyl-5β-androstane-3α,17β-diol (**3.0**), 17α-methyl-5β-androstane-3β,17β-diol (**4.0**), 19,19,19-d₃-17α-methyl-5α-androstane-3β,17β-diol (**2.4**), 19,19,19-d₃-17α-methyl-5β-androstane-3β,17β-diol (**4.4**), 20,20,20-d₃-17α-methyl-5α-androstane-3β,17β-diol (**2.5**), 20,20,20-d₃-17α-methyl-5β-androstane-3α,17β-diol (**3.5**), 20,20,20-d₃-17α-methyl-5β-androstane-3β,17β-diol (**4.5**),

FIGURE 2 (A) Chemical structures of unlabeled bis-TMS derivatives of THMT isomers mentioned in Section 2.1.1. (B) Schematic depiction of structures of synthesized and examined isotopologues without stereochemical descriptors visualizing site of deuteration including resulting mass shift of the bis-TMS derivatives of THMT (with "#" representing corresponding core structure of non-derivatized THMT **1.0**, **2.0**, **3.0**, or **4.0**).

16,16-d$_2$-17α-methyl-5α-androstane-3α,17β-diol (**1.6**), 16,16-d$_2$-17α-methyl-5α-androstane-3β,17β-diol (**2.6**), 16,16-d$_2$-17α-methyl-5β-androstane-3α,17β-diol (**3.6**), 16,16-d$_2$-17α-methyl-5β-androstane-3β,17β-diol (**4.6**), 2,2,3,4,4-d$_5$-17α-methyl-5α-androstane-3α,17β-diol (**1.7**), 5-d$_1$-17α-methyl-5α-androstane-17β,3β-ol (**2.9**), 5-d$_1$-17α-methyl-5β-androstane-17β,3α-ol (**3.9**), 5-d$_1$-17α-methyl-5β-androstane-17β,3β-ol (**4.9**). Detailed procedures of synthesis and structural confirmation are published in a public data repository: https://doi.org/10.17169/refubium-42842.

2.1.1 | Systematical derivatization of THMT diastereomers

Unlabeled 3,17-bis-TMS derivatives resulted when 10 μg of reference compounds were treated with 100 μL of a solution of MSTFA, NH$_4$I and ethanethiol (1000:2:3, v/w/v).

3,17-[^{2}H$_9$]-bis-TMS derivatives were generated by incubating aliquots of 10 μg of respective THMT isomer with 11 μL of [^{2}H$_{18}$]-N,O-bis[trimethylsilyl]acetamide (d$_{18}$-BSA) at 90°C for 30 min. The liquid was brought to dryness with a gentle stream of nitrogen and was redissolved in 50 μL of cyclohexane.

Mixed 3-TMS-17-[^{2}H$_9$]-TMS derivatives were obtained in accordance with 3,17-[^{2}H$_9$]-bis-TMS derivatives, but prior to incubation with [^{2}H$_{18}$]-BSA 50 μL of MSTFA was added and incubated at 75°C for 15 min and then evaporated.

2.2 | Instrumentation

2.2.1 | GC/MS

Low-resolution GC/EI-MS experiments were conducted on a 7890 gas chromatograph (Agilent Technologies Inc., Santa Clara, CA, USA) hyphenated to a 5975C single quadrupole mass-selective detector (Agilent Technologies Inc.). A HP-Ultra 1 column (17 m × 200 μm ×

0.11 μm; Agilent Technologies Inc.) was used with helium as carrier gas with a constant flow rate of 1 mL/min. Inlet temperature was 300°C, injection volume 2 μL and split ratio 25:1. The oven temperature started at 183°C heating 3°C/min up to 232°C and then heated 40°C/min to 310°C with a hold time of 2 min. Ionization energy of 70 eV was applied and full scan mode ranged from m/z 40 to 1000.

To improve chromatographic separation from side products during analysis of synthesis of 19,19,19-d$_3$-THMT structures an adjusted method was used. It also started at 183°C and increased the temperature with 5°C/min up to 200°C. After a hold time of 10 min a ramp of 3°C/min up to 215°C was added and then heated with 40°C/min up to 310°C with a hold time of 2 min. Other conditions were kept equal.

2.2.2 | GC/QTOF-MS

High-resolution data was acquired on an Agilent GC/EI-QTOF-MS 7890B/7250 (Agilent Technologies Inc., Milano, Italy) equipped with a HP-5MS capillary column (17 m × 200 μm × 0.11 μm, Agilent Technologies Inc.). Differences from the method used above (Section 2.2.1) is inlet temperature of 280°C, split ratio of 10:1, constant pressure of 18 psi and following oven parameters: initial setpoint 150°C, heating rate of 50°C/min up to 200°C, following heating of 3°C/min up to 230°C, heating rate of 50°C/min up to 320°C and a final hold time for 3 min. The coupled QTOF mass spectrometer was operated in full scan mode with an ionization energy of 70 eV and range from m/z 50 to 750. Mass calibration was performed twice prior to every sequence and then repeated after every second injection.

2.3 | Statistical comparison of relative intensities of EI fragment ions

Mean intensities of identical fragment ions of four isomeric THMTs were compared among each other to later contextualize with

respective stereochemistry. These substances were measured multiple times ($n = 5$) with GC/EI-QTOF-MS as technical replicates. Using Agilent MassHunter Qualitative Analysis 10.0 (Agilent Technologies) the spectra of apexes of the chromatographic peaks were extracted and subsequently the background has been subtracted. Intensities of fragment ions were normalized to the base peak intensity (m/z 143) and exported for further statistical analysis to OriginPro 2021b (OriginLab Corporation, Northhampton, MA, USA). Firstly, Shapiro–Wilk test for normal distribution was performed and if normal distribution was not confirmed Grubbs test for outliers was added. If set of data was normally distributed and homogeneity of variances was proven by Levenes test an analysis of variances was conducted. If there was significant difference between the groups, Tukey post-hoc test was used for further description. In case of normal distribution and heterogeneity of variances Welch-ANOVA and a Games-Howell pairwise comparison was method of choice. Significance level of all tests were chosen as $\alpha = 0.05$.

3 | RESULTS AND DISCUSSION

3.1 | Labelled TMS derivatives of THMT diastereomers

To obtain selectively labelled hydroxy groups at C3 and C17 varying silylating power and steric circumstances was taken advantage of.[13] Due to the sterically hindered hydroxy group at C17 pure MSTFA mainly silylates the hydroxy group at C3. In comparison, TMSI and BSA are able to derivatize C3 and C17.[28] Perdeuterotrimethylsilyl was introduced by [^{2}H$_{18}$]-BSA.[22,24] Mass spectra of **2.1**, **2.2**, and **2.3** are exemplary depicted in Figure 3, and GC/EI-MS spectra of **1.1**, **2.1**, **3.1**, and **4.1** are available from the supporting information (Supplement I).

In the following isotopologues of THMT with configurations in the A-ring analogous to androsterone (3α5α), epiandrosterone (3β5α), etiocholanolone (3α5β), and epietiocholanolone (3β5β) will be referred
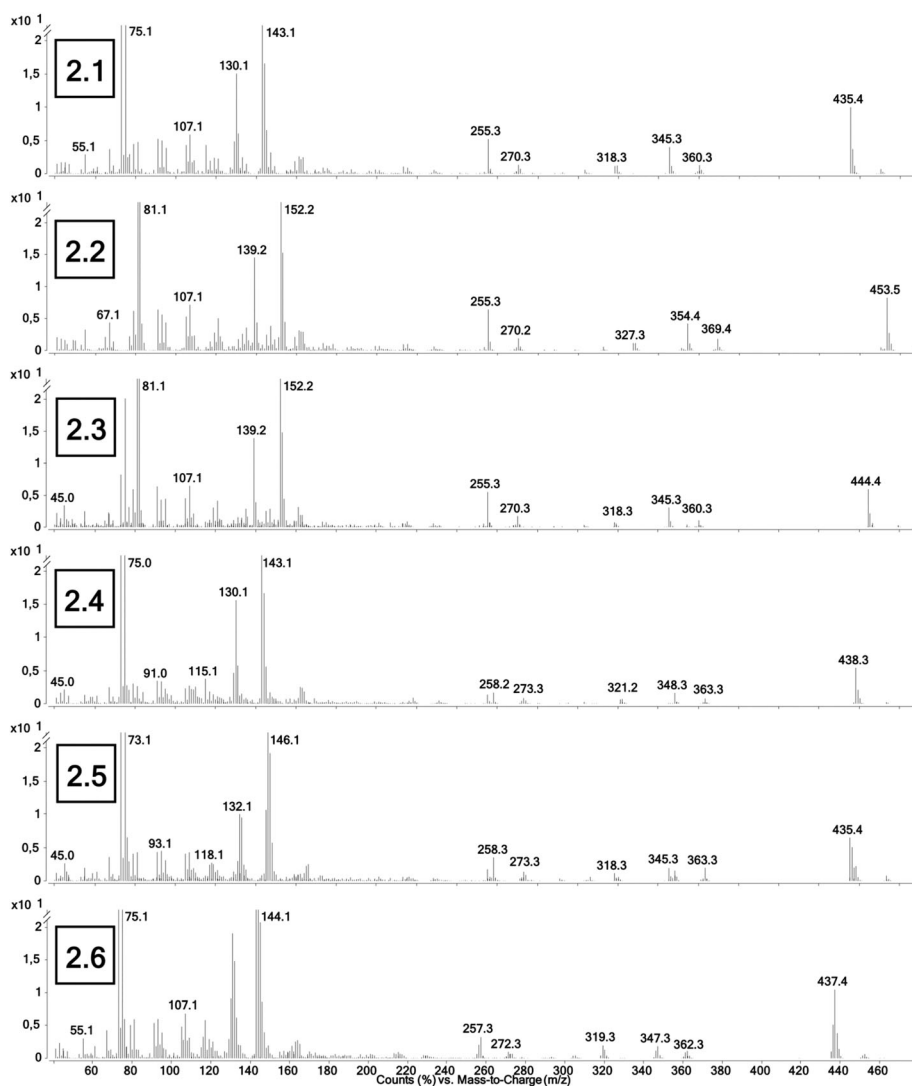
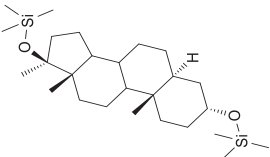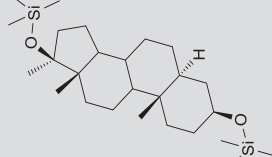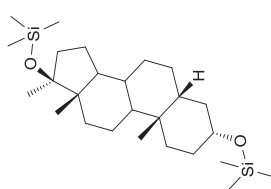**FIGURE 3** Zoomed in part of GC/MS spectra of MEA derivatives normalized to base peak m/z 143 3,17-bis-TMS (**2.1**), 3,17-[^{2}H$_9$]-bis-TMS (**2.2**), 3-TMS-17-[^{2}H$_9$]-TMS (**2.3**), 19,19,19-d$_3$–3,17-bis-TMS (**2.4**), 20,20,20-d$_3$–3,17-bis-TMS (**2.5**), and 16,16-d$_2$-bis-TMS (**2.6**).

TABLE 1 Experimental data of GC/MS fragment ions of standards 1–4.

Number	Ion	#1: 3,17-bis-TMS	#2: 3,17-[^{2}H$_9$]-bis-TMS	#3: 3-TMS, 17-[^{2}H$_9$]-TMS	#4: 19,19,19-d_3-3,17-bis-TMS	#5: 20,20,20-d_3-3,17-bis-TMS	#6: 16,16-d_2-bis-TMS	1.7: 2,2,3,4,4-d_5-bis-TMS	1.8: 3-[^{2}H$_9$]-bis-TMS
1 MA	[M]$^{\bullet+}$	450.4	468.5	459.5	453.3	453.4	452.4	455.4	459.4
	[M-CH$_3$]$^+$	435.4	453.5; 450.4 (7%)	444.4	438.8	435.4 (75%); 438.4 (25%)	437.4	440.4	444.4 (98%); 441.4 (2%)
	[M-90]$^{\bullet+}$ / [M-99]$^{\bullet+}$	360.3	369.4	360.4	363.3	363.3	362.3	365.3	369.4
	[M-90-CH$_3$]$^+$ [M-90-CD$_3$]$^+$ [M-99-CH$_3$]$^+$ [M-99-CD$_3$]$^+$	345.3	354.4 (89%); 351.3 (11%)	354.3 (23%); 345.3 (77%)	348.3	348.3 (44%); 345.3 (56%)		350.3	354.4 (62%); 345.3 (38%)
	[M-132]$^{\bullet+}$	318.3	327.3	318.2	321.2	318.3	320.3	323.3	327.3
	[M-2x90]$^{\bullet+}$ / [M-2x99]$^{\bullet+}$ / [M-90-99]$^{\bullet+}$	270.3	270.3	270.2	273.3	273.3	272.3	275.3	270.3
	[M-2x90-CH$_3$]$^+$ / [M-2x99-CH$_3$]$^+$ / [M-90-99-CH$_3$]$^+$	255.3	255.3	255.2	258.2	255.2 (33%); 258.3 (67%)	257.3	260.3	255.2
	D-ring	143.1	152.2	152.2	143.1	146.1	144.1 (55%); 143.1 (45%)	143.1	143.1
2 MEA	[M]$^{\bullet+}$	450.4	468.5	459.4	453.3	453.4	452.4		
	[M-CH$_3$]$^{\bullet+}$ [M-CD$_3$]$^+$	435.4	453.5 (93%); 450.4 (7%)	444.4	438.8	435.4 (75%); 438.4 (25%)	437.4		
	[M-90]$^{\bullet+}$ / [M-99]$^{\bullet+}$	360.3	369.4	360.3	363.3	363.3	362.3		
	[M-90-CH$_3$]$^+$ [M-90-CD$_3$]$^+$ [M-99-CH$_3$]$^+$ [M-99-CD$_3$]$^+$	345.3	354.3 (89%); 351.4 (11%)	354.4 (11%); 345.3 (89%)	348.3	348.3 (44%); 345.3 (56%)			
	[M-132]$^{\bullet+}$	318.3	327.3	318.3	321.2	318.3	320.3		
	[M-2x90]$^{\bullet+}$ / [M-2x99]$^{\bullet+}$	270.3	270.2	270.3	273.3	273.3	272.3		
	[M-2x90-CH$_3$]$^+$ / [M-2x99-CH$_3$]$^+$ / [M-90-99-CH$_3$]$^+$ / [M-2x90-CD$_3$]$^+$	255.3	255.3	255.3	258.2	255.2 (33%); 258.3 (67%)	257.3		
	D-ring	143.1	152.2	152.2	143.1	146.1	144.1 (56%); 143.1 (44%)		
3 ME	[M]$^{\bullet+}$	450.4	468.5	459.4		453.4	452.4		
	[M-CH$_3$]$^+$	435.4	453.5 (95%)	444.4		438.4 (25%)	437.4		

(Continues)

TABLE 1 (Continued)

Structure 1 (top): 3,17-bis-TMS diol (3-OTMS epimer) — continued

Ion	#1: 3,17-bis-TMS	#2: 3,17-$[^2H_9]$-bis-TMS	#3: 3-TMS, 17-$[^2H_9]$-TMS	#4: 19,19,19-d_3-3,17-bis-TMS	#5: 20,20,20-d_3-3,17-bis-TMS	#6: 16,16-d_2-bis-TMS	1.7: 2,2,3,4,4-d_5-bis-TMS	1.8: 3-$[^2H_9]$-bis-TMS
$[M-CD_3]^+$		450.4 (5%)			435.4 (75%)			
$[M-90]^{\bullet+}/[M-99]^{\bullet+}$	360.3	369.5	360.3	363.4	363.3	362.3		
$[M-90-CH_3]^+$	345.3	354.3 (86%)	354.4 (66%)	348.3	348.3 (20%)			
$[M-90-CD_3]^+$ / $[M-99-CH_3]^+$ / $[M-99-CD_3]^+$		351.3 (14%)	351.3 (5%) / 345.3 (29%)		345.3 (80%)			
$[M-132]^{\bullet+}$	318.3	327.3	327.3	321.2	318.3	320.3		
$[M-2x90]^{\bullet+}/[M-2x99]^{\bullet+}$	270.3	270.3	270.3	273.2	273.3	272.3		
$[M-2x90-CH_3]^+$ / $[M-2x99-CH_3]^+$ / $[M-90-99-CH_3]^+$ / $[M-2x90-CD_3]^+$	255.3	255.2	255.3	258.2 (49%) / 255.2 (51%)	258.3 (70%) / 255.3 (30%)	257.3		
D-ring	143.1	152.2	152.2	143.1	146.2	144.1 (57%) / 143.1 (43%)		

Structure 4: MEE (3-OTMS epimer)

Number	Ion	#1: 3,17-bis-TMS	#2: 3,17-$[^2H_9]$-bis-TMS	#3: 3-TMS, 17-$[^2H_9]$-TMS	#4: 19,19,19-d_3-3,17-bis-TMS	#5: 20,20,20-d_3-3,17-bis-TMS	#6: 16,16-d_2-bis-TMS	1.7: 2,2,3,4,4-d_5-bis-TMS	1.8: 3-$[^2H_9]$-bis-TMS
4	$[M]^{\bullet+}$	450.4	468.5	459.5	453.4	452.4	452.4		
	$[M-CH_3]^+$ / $[M-CD_3]^+$	435.4	453.5 (97%) / 450.5 (3%)	444.4	438.4	438.4 (17%) / 435.4 (83%)	437.4		
	$[M-90]^{\bullet+}/[M-99]^{\bullet+}$	360.3	369.4	369.3 (22%) / 360.3 (78%)	363.4	363.3	362.3		
	$[M-90-CH_3]^+$	345.3	354.4 (94%)	354.3 (65%)	348.3	348.3 (33%)			
	$[M-90-CD_3]^+$ / $[M-99-CH_3]^+$ / $[M-99-CD_3]^+$		351.3 (6%)	351.3 (2%) / 345.3 (33%)		345.3 (67%)			
	$[M-132]^{\bullet+}$	318.3	327.3	318.2	321.2	318.3	320.3		
	$[M-2x90]^{\bullet+}/[M-2x99]^{\bullet+}$	270.3	270.3	270.3	273.2	273.3	272.3		
	$[M-2x90-CH_3]^+$ / $[M-2x99-CH_3]^+$ / $[M-90-99-CH_3]^+$ / $[M-2x90-CD_3]^+$	255.3	255.3	255.2	258.2 (49%) / 255.2 (51%)	258.3 (67%) / 255.3 (33%)	257.3		
	D-ring	143.1	152.2	152.2	143.1	146.1	144.1 (54%) / 143.1 (46%)		

%Values given in brackets represent contribution of the individual isotopologue fragment ions to the total abundance of the corresponding fragment ion of the unlabeled isotopologue.

Abbreviations: $[M-90]^{\bullet+}$ = $[M-TMSOH]^{\bullet+}$, $[M-99]^{\bullet+}$ = $[M-[^2H_9]-TMSOH]^{\bullet+}$, $[M-90-CH_3]^+$ = $[M-TMSOH-CH_3]^+$, $[M-90-CD_3]^+$ = $[M-TMSOH-CD_3]^+$, $[M-99-CH_3]^+$ = $[M-[^2H_9]-TMSOH-CH_3]^+$, $[M-99-CD_3]^+$ = $[M-[^2H_9]-TMSOH-CD_3]^+$, $[M-2x90]^{\bullet+}$ = $[M-2xTMSOH]^{\bullet+}$, $[M-2x99]^{\bullet+}$ = $[M-2x[^2H_9]-TMSOH]^{\bullet+}$, $[M-90-99]^{\bullet+}$ = $[M-TMSOH-[^2H_9]-TMSOH]^{\bullet+}$, $[M-90-99]^{\bullet+}$ = $[M-TMSOH-[^2H_9]-TMSOH]^{\bullet+}$, $[M-2x90-CH_3]^+$ = $[M-2xTMSOH-CH_3]^+$, $[M-2x99-CH_3]^+$ = $[M-2xTMSOH-CH_3]^+$, $[M-2x90-CD_3]^+$ = $[M-2x[^2H_9]-TMSOH-CH_3]^+$, $[M-90-99-CH_3]^+$ = $[M-TMSOH - [^2H_9]-TMSOH-CH_3]^+$.

to as MA, MEA, ME, and MEE as depicted in Figure 2A. The percentages stated in brackets in combination to these abbreviations originate from Table 1 as contribution of the labelled isotopologues fragment ion to the corresponding fragment ion with labelled substructures. If a stereoisomer is not mentioned, then there is no according data available due to a lack of reference material.
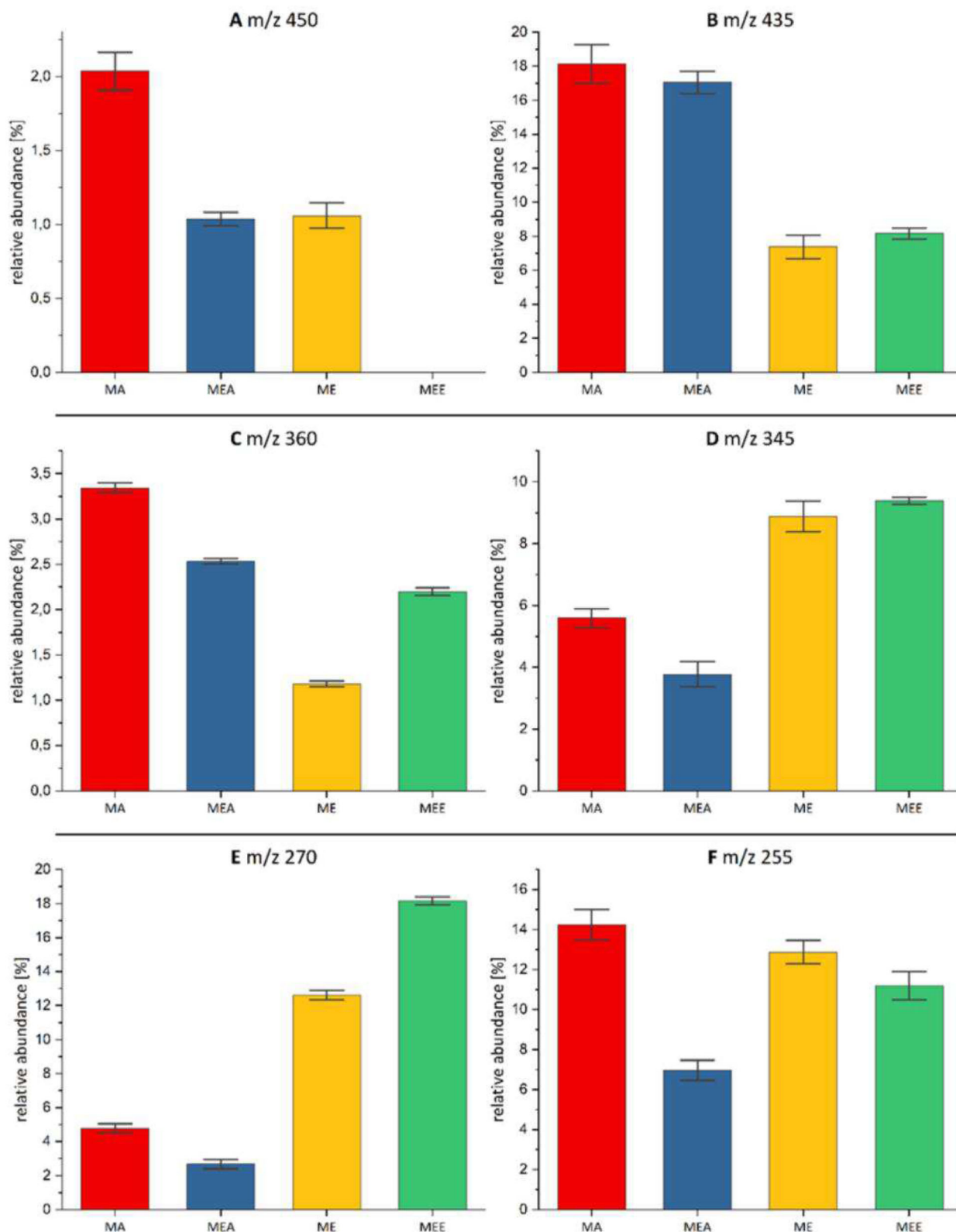

FIGURE 4 Mean relative abundance relative to *m/z* 143 of GC/MS fragment ions of repeated measurements (*n* = 5) of 1.1 to 4.1 as described in Section 2.4. [Color figure can be viewed at wileyonlinelibrary.com]

3.2 | Molecular ion [M]$^{\bullet+}$

Electron ionization belongs to the group of hard ionizations and that often leads to low abundances of the molecular radical cation, also in this case, $[M]^{\bullet+} = m/z$ 450 as illustrated in Figure 4A. The abundance of molecular radical cation of MEE was not even quantifiable. MA shows a significantly higher relative abundance compared to ME and MEA, which indicates a higher thermodynamic stability of this ion.

3.3 | Fragment ion [M-CH$_3$]$^+$

The loss of 15 Da in unlabeled structures indicates a radical loss of a methyl group. In these molecules, it might either emerge from the steroid nucleus from C18, C19, or C20 or from the TMS groups in position C3 or C17. By selectively labelling single substructures as for example the methyl group at C20 as in **2.5**, **3.5**, and **4.5** the mass of fragment ions is shifted by +3 Da which enables deduction to which fragment ion a substructure contributes in comparison to spectra of unlabeled molecules. For this reason, abundances of losses of 15 Da compared with 18 Da to yield fragments obtained from 3,17-[^{2}H$_9$]-bis-TMS isomers with 3-TMS,17-[^{2}H$_9$]-TMS isomers show that only a minor contribution to fragment signals is derived from a cleavage at TMS groups (MA 2%, MEA 7%, ME 5%, MEE 3%). Furthermore, in all four isomers, if cleaved from TMS groups, loss takes places from TMS at C3. Consequentially, main loss of the methyl group originates from the steroid backbone. A loss of 18 Da in 20,20,20-d$_3$-THMT isomers (MEA 75%, ME 75%, MEE 83%) confirms that losses of methyl groups from the steroid nucleus majorily originate from C20. In addition, only losses of 15 Da and no loss of 18 Da in 19,19,19-d$_3$-THMT isomers led to the conclusion that the loss of the C18-methyl group contributes to the formation of [M−CH$_3$]$^+$ besides the loss of C20 (MEA 25%, MEE 17%). No significant impact by the stereochemistry of the A-ring was observed for the generation of these fragments, which is in line with the observation that the loss of a methyl group mainly takes place at the D-ring.

However, comparison of relative abundances among MA, MEA, ME, and MEE in Figure 4B shows significant differences even if composition of contributing fragments as shown above is very similar. 5α-Configuration shows abundances at least twice as high as 5β-configuration, which might indicate a higher stability of fragment ions with 5α-configuration. Interestingly, the same observation was made by Massé et al investigating, inter alia, mono-TMS and bis-TMS derivatives of 19-norandrosterone, 19-norepiandrosterone, 19-noretiocholanolone, and 19-norepietiocholanolone.[17]

Fascinatingly, comparing this data with findings of Kollmeier et al. about 5ξ-androstane-3ξ,17β-diols shows highly significant divergence of fragmentational behavior by the additional 17α-methyl group. Without a 17α-methyl group these molecules show up to 90% of the cleavage from TMS groups.[22] In THMT, it shifts almost completely to a loss of C20- or C18-methyl group. Further, it has been reported that 17α-methyl-androst-5-ene-3β,17β-diol yields the fragment ion

[M-CH$_3$]$^+$ with 60% representing elimination of the 17α-methyl group and 40% being cleaved from 3β-TMS function.[12] The assignment of 60% of elimination to 17α-methyl group as sole origin by Vouros et al. must be evaluated critically because it does not include C18 and C19 as possible origin especially when having only spectral data of 3,17-[^{2}H$_9$]-bis-TMS derivatives.

3.4 | Fragment ion [M-TMSOH]$^{\bullet+}$

The fragment ion m/z 360 evolves after a loss of 90 Da, which is known as cleavage of a TMSO group with an additional hydrogen (TMSOH). It was shown by Kollmeier et al. and Fenselau et al. that hydrogens in 1,3-diaxial position to the TMS group are favored to be eliminated presumably due to their intramolecular distance with TMSO.[22,29] As [M−TMSOH]$^{\bullet+}$ represents the loss of a group which was added via derivatization in sample preparation only little structural information is allegedly delivered. Comparing abundances of [M−90]$^{\bullet+}$ and [M−99]$^{\bullet+}$ in 3-TMS,17-[^{2}H$_9$]-TMS isomers shows that cleavage of TMSOH in MA, MEA, and ME exclusively appears at C17. Only MEE shows an additional cleavage from C3 of about 22%.

In Kollmeier et al.'s work, 5ξ-androstane-3ξ,17β-diols, similar to THMT without a 17α-methyl group, show that 5α-configuration supports cleavage of TMSOH from C17. Equivalent to this, diastereomers with 5β-configuration cleavage from C3 is favored. In contrast, THMT diastereomers show overall behavior of cleaving TMSOH from C17 and only MEE showing partially cleavage from C3. This may be explained by structural tension resulting from the joint methyl group and the TMSO group at C17 generally favoring the cleavage at C17. However, in case of MEE, the TMSO group at C3 in 1,3-diaxial position is in favorable distance with H5 which supports the loss of TMSOH as shown by Kollmeier et al., whereas MA, MEA, and ME do not exhibit this favorable distance.[22]

The deuteration in case of 16,16-d$_2$-derivatives was not quantitative. Therefore, signals with a mass shift of $m/z + 2$ and $m/z + 1$ are detectable in considerable amounts and statements about the elimination of a single hydrogen at position 16 during fragmentation are not robust.

3.5 | Fragment ion [M-CH$_3$-TMSOH]$^+$

The composition of fragment ion m/z 345 shows a variety of compositions due to losses of methyl and TMS groups and combinations among them from different positions. Overall, about 90% of the methyl group cleavages originate from the steroid backbone and not from the remaining TMS group as described in Section 3.3. The majority of these 90% originates again from C20 (MEA 56%, ME 80%, MEE 67%) and minorly from C18 (MEA 44%, MEE 33%). No loss of the C19-methyl group was observed. Interestingly, in this fragment the origin of cleavage of TMSOH follows the same pattern as in the 5ξ-androstane-3ξ,17β-diols.[22] In detail, 5α-configuration results in an excessive cleavage at C17

(MA 62–77%, MEA 89%) and 5β isomers mainly eliminate TMSOH from C3 (ME 71%, MEE 67%). Thus, a loss of 105 Da in 3-TMS,17-[^{2}H$_9$]TMS isomers in ME and MEE indicates that the loss of the methyl group originates from backbone and TMSOH is cleaved from C3. Comparing abundances to the loss of 108 Da (cleavage of a methyl group from TMS group at C17 instead) allows following statement: If TMSOH originates from C3, the methyl group originates excessively from steroid nucleus (ME93%, MEE97%). This knowledge supports the hypothesis that [M-CH$_3$ -TMSOH]$^+$ is formed sequentially by a first loss of the methyl group, preferably C20, as the fragmentation behavior in this case is very similar to Kollmeier et al.'s findings referring to the origin of TMSOH in 5α and 5β-configuration. This thesis is further strengthened when structural similarities of 5ξ-androstane-3ξ,17β-diols to the fragment [M-CH$_3$]$^+$ of THMTs are considered. Additionally, the amounts of cleaved methyl group C20 (ME 80% and MEE 67%) are very similar to the amounts of eliminated TMSOH from C3 (ME 71%, MEE 67%). The same pattern was seen with methyl group C18 (ME 20%, MEE 33%) and eliminated TMSOH from C17 (ME 29%, MEE 33%). This data supports the hypothesis that cleavage of two groups at the same position as C17 is unfavored. Thus, if TMSOH is cleaved from C17, the C20-methyl group will not be eliminated but rather C18 methyl.

In case of 5β-configuration, TMSOH is mainly cleaved from C3 and the majority of methyl group losses derive from C20. Now taking relative abundances into consideration, 5β-configuration shows significantly higher intensities of [M-CH$_3$-TMSOH]$^+$ than 5α (Figure 4D). Hence, it seems as it is energetically favored that cleavage happens at C3 and C20 (5β-configuration) than at C17 and C18 (5α-configuration).

3.6 | Fragment ion [M-2xTMSOH]$^{•+}$

In unlabeled molecules of THMT derivatized with TMIS the fragment ion m/z 270 represents the structure after the loss of the two TMSOH residues. Therefore, no assignment of origin needs to be done. Interestingly, relative abundances of m/z 270 show significant differences among MA, MEA, ME and MEE even though 5α-configuration displays again noticeably lower signals than 5β-configuration (Figure 4E). Considering that this preference was observed before for ion [M-CH$_3$-TMSOH]$^+$ where 5β preferably leads to cleavage of TMSOH at C3 in combination with the C20-methyl group, it might be the case that the preference of cleaving TMSOH from C3 does not depend on loss of 17α methyl but mainly depends on configuration of the hydroxy group at C3.

Regarding the fact that m/z 360 represents the loss of a single TMSOH, which is almost without exception located at C17 (3.4), it seems as the formation of the fragment m/z 270 depends on favorability of cleavage from C3. But contemplating the relative abundances among the isomers of THMT, no preference towards 3α- or 3β-configuration of the hydroxy group can be noted (Figure 4C). Although the validity of statements about the loss of a hydrogen in position 16 is limited due to the isotopic purity of the isotopologues,

the fragment ion [M-2xTMSOH]$^{•+}$ of 16,16-d$_2$-isotopologues shows a shift of the ratio between m/z 271 and m/z 272 towards m/z 271. This may imply an elimination of a 16D and therefore explain the origin of the deuterium contributing to the cleavage of a TMSOD. This hypothesis can be supported by the intramolecular distance between 16D and the oxygen of the TMS group.[22,29] Furthermore, fragmentation of 18,18,18-d$_3$-THMT could give illuminating insights to the origin of the hydrogen, when TMSOH is cleaved from C17 and will therefore be addressed in future investigations.

3.7 | Fragment ion [M-CH$_3$-2xTMSOH]$^+$

The loss of two TMSOH and one methyl group is represented by the fragment ion m/z 255 in unlabeled molecules of derivatized THMT. After loss of all TMSOH the origin of the methyl group must be from the steroid backbone. Contrasting 19,19,19-d$_3$-3,17-bis-TMS and 20,20,20-d$_3$-3,17-bis-TMS in Table 1 revealed that in this fragment the majority of methyl losses derives from C19 (MEA 45%, MEE 51%) and about one third from C20 (MEA 33%, ME 30%, MEE 33%). Due to a lack of 19,19,19-d$_3$-ME (**3.4**), it can only be stated that 70% derive from C19 or C18 which indicates similar behavior as MEA and MEE. This leads to the impression that stereochemistry has a rather minor impact on the proportion of origin of the methyl group in this fragment.

Not only is C19 the major origin of cleaved methyl groups in m/z 255 but it is also interestingly the very first fragment showing a loss at this position at all. At least for MEA and ME and their corresponding fragment signals of [M-CH$_3$]$^+$ and [M-CH$_3$-TMSOH]$^+$ as source of fragmentation C19 was not observed. This either indicates that as long as there is a TMS group remaining in the molecule, it is highly unfavored to cleave off C19 and m/z 255 does mainly not originate from m/z 435. Or on the other hand, it can also suggest that fragment ions m/z 435 resulting of a loss of C19 are simply not detectable, because of very fast elimination of two TMSOH groups.

Furthermore, 5-d$_1$-isomers of MEA, ME, and MEE were obtained and elimination tendency of hydrogen atoms in 1,3-diaxial position to a TMSO group was evaluated. Respective mass spectra are depicted in Figure 5. Theoretically, hydrogen at C1 and C5 are in 1,3-diaxial position to a TMSO group. For MEA and ME the formation of m/z 256, same as m/z 346 and m/z 271, indicating the remaining of 5D in the molecule, were observed. In contrast, for MEE additional signals in considerable intensities of m/z 255, m/z 345 and m/z 270 were detected. This finding is in line with Kollmeier et al.'s hypothesis for TMSO group in 3β and hydrogen in 5β position where a 1,3-diaxial position in adequate bonding distance is supporting elimination of a 5β deuterium atom for the loss of TMSOD fragments.[22,29] In theory, in MEA and MEE with a TMSO group in 3β configuration the 1β hydrogen is also in a favorable distance for the elimination of TMSOH. On the other hand, in MA and ME with a TMSO group in 3α configuration, it seems more likely for the protons in 1α position to be eliminated as well.
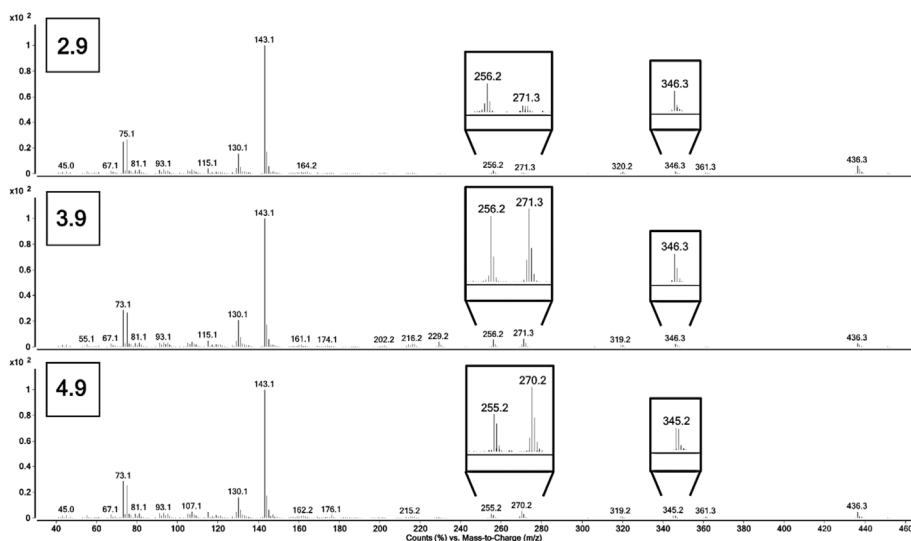
FIGURE 5 GC/MS spectra of 5-d$_1$-isomers: **2.9** (MEA), **3.9** (ME), and **4.9** (MEE).
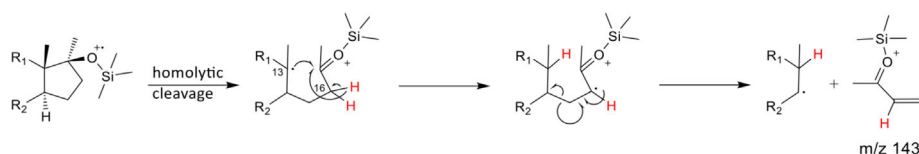

FIGURE 6 Proposed mechanism of formation of m/z 143 by Borges et al. [Color figure can be viewed at wileyonlinelibrary.com]

Furthermore, MEA shows a significantly lower relative intensity for the loss of TMSOH compared to the other three isomers (Figure 4F). This may be explained by a lack of hydrogen atoms in 1,3-diaxial position to the TMS group in 3α position or in general spatial proximity as it is the case for ME with hydrogens in 7α and 9 position.[22]

3.8 | Fragment ion m/z 143

Even though relative intensities vary between the investigated stereoisomers, m/z 143 always represents the base peak. This fragment ion is very characteristic for 17α-methyl steroids and is therefore used as indicator in anti-doping analysis for trimethylsilylated 17α-methyl steroids.[30] It must be noted that m/z 143 may also result from several steroid structures, such as 3-hydroxy steroids with a double bond within the A-ring or some with vicinal TMSO groups like 5α-androstane-2β,3α,17β-triol.[31-33] Interestingly, 3ξ,4ξ-dihydroxy-5ξ-androstan-17-ones or 3α,4β,7α-trihydroxy-5β-cholanoic acid provide the fragment m/z 147.[34,35] The fragment ion in spectra of THMT generally originates from the D-ring and a mechanism of formation has been postulated.[11,12,36,37] m/z 143, m/z 146 and m/z 152 in the different isotopologues of our investigations further confirmed that mechanism (Figure 6). It has been reported that if a methyl or an ethyl group was introduced to C17 of an AAS, predominantly the respective D-ring fragment appears to result as the base peak.[19] By normalizing investigated spectra to the abundance of m/z 143 one must be aware that even if it is common

practice every value of relative intensity is influenced by the abundance of m/z 143 and statements according to m/z 143 and for comparison among stereoisomers is not possible in this case. Therefore, all obtained spectra were additionally normalized to the intensity of the total ion current (TIC). This gives us a new possibility to assess the impact of variations in absolute abundances of m/z 143 among the four diastereomers. The overall procedure was as described in Section 2.3, except not using apexes but integrated peaks to extract mass spectra. The figure of the resulting data is available from the supporting information (Supplement II). Even though the abundance of m/z 143 varies, the impact on the relative abundance of the investigated fragment ions (m/z 450, m/z 435, m/z 360, m/z 345 m/z 270, m/z 255) and the ratio of relative abundances is consistent. Thus, the quality of the statements based on this data is not impacted. Moreover, what makes it even more challenging to describe m/z 143 is that the remaining steroid backbone with a theoretical signal m/z 307 due to a potential neutral loss of C15-C17 is not observed. The partial shift from m/z 143 to m/z 144 in the 16,16-d$_2$-isomers (**2.6**, Table 1) leads to the theory that there must be more than one origin of formation of this fragment ion. Regarding the proposed mechanism of formation by Borges et al. which also proclaims formation of a bond between C13 and one proton of C16, m/z 144 can be explained (Figure 6).[37] But there is still a lack of explanation for the formation of the signal m/z 143 of these 16,16-d$_2$-isomers with a ratio of intensity of about 55:45 compared with m/z 144. This may indicate that there is a parallel second way of formation involving a loss of both deuterium atoms at C16 or that the formation includes an enol intermediate after the homolytic cleavage (Figure 6).
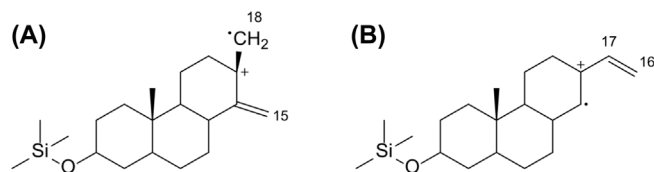
(A) **(B)**

FIGURE 7 Possible postulated structures of fragment ion m/z 318 (m_e = 318.2373, $C_{20}H_{34}OSi^+$).

TABLE 2 Stereochemical assignment, accurate mass and mass difference of a fragment ion m/z 318 ($M^{\bullet+}$, EI, 70 eV), mean (n = 5) mass difference to exact mass (m_e = 318.2373, $C_{20}H_{34}OSi^{\bullet+}$, as mono-TMS derivatives).

Stereochemical assignment	Accurate mass	Δ m/z (ppm)
3α5α/MA	318.2374	0.31
3β5α/MEA	318.2376	0.94
3α5β/ME	318.2376	0.94
3β5β/MEE	318.2378	1.57

3.9 | Fragment ion m/z 318

m/z 318 has been reported for 3,17-bis-TMS derivatives of THMT before, but was not yet further described structurally.[12] This fragment may be explained by the cleavage of the C-13/C-17 and C-15/C-16 bonds and an additional elimination of two hydrogens resulting in a postulated fragment ion as illustrated in Figure 7A, in analogy to the fragment ion, m/z 246, derived from androsterone, epiandrosterone, etiocholanolone, and epietiocholanolone. This was described for underivatized samples by Egger et al. and supported using stable isotopic labeling.[38] Moreover, labeling experiments of our work (see Table 1) have shown that the TMS group at C3 and methyl group at C19 remain in this fragment whereas the TMS group at C17 and C20-methyl group are cleaved off. Furthermore, 2,2,3,4,4-d_5-THMT (**1.7**) showed no loss of labeled positions. On the other hand, spectra of 16,16-d_2-isomers show a fragment ion m/z 320, which indicates remaining of the labeled position. Thus, it might be better explained by the proposal given in Figure 7B. The average mass error among the four stereoisomers of THMT (Table 2) supports the proposed elemental composition of $C_{20}H_{34}OSi^+$ which is identical for both structure proposals. To further elucidate the structure of this fragment the mass spectra of 18,18,18-d_3-THMT would be of eminent importance to see if a mass shift of m/z 318 + 2 or a loss of 18 Da will be detectable. This will be addressed in future investigations.

4 | CONCLUSION

This work was able to point out clear differences in fragmentation pattern of the four diastereomers MA, MEA, ME, and MEE. Not only relative intensities diverge among these isomers but also the compositions of single signals are different. It was achieved to assign structural origins of fragment ions m/z 435, m/z 360, m/z 345, m/z 270, m/z 255 and to give semi-quantitative statements about the contribution of the different origins for methyl and TMS groups. This demonstrated crucial differences between THMTs and their 20-nor analogues 5ξ-androstane-3ξ,17β-diols in the composition of the respective ions [M-TMSOH]$^{\bullet+}$ and [M-CH$_3$]$^+$. The latter were investigated by our group previously and a fundamental shift of favored origin of cleaved methyl groups was observed. This nicely illustrates that even allegedly minor structural variations as the 17α-methyl group can significantly impact fragmentation patterns. On the other hand, the previous hypothesis of Kollmeier et al. was confirmed that for MEE a 1,3-diaxial configuration of TMSOH in 3β and hydrogen atom in 5β position supports elimination of TMSOH from the A-ring. Additionally, two previously unknown structures for a yet uncharacterized fragment ion were proposed and supported by HRMS measurements.

ORCID

Jakob Steff https://orcid.org/0009-0009-0330-3131
Maria K. Parr https://orcid.org/0000-0001-7407-8300

REFERENCES

1. Stein S. Mass spectral reference libraries: an ever-expanding resource for chemical identification. *Anal Chem*. 2012;84(17):7274-7282. doi:10.1021/ac301205z
2. Stein SE. Estimating probabilities of correct identification from results of mass spectral library searches. *J Am Soc Mass Spectrom*. 1994;5(4):316-323. doi:10.1016/1044-0305(94)85022-4
3. Wallace WE, Ji W, Tchekhovskoi DV, Phinney KW, Stein SE. Mass spectral library quality assurance by inter-library comparison. *J Am Soc Mass Spectrom*. 2017;28(4):733-738. doi:10.1007/s13361-016-1589-4

4. Meyerson S, Weitkamp AW. Stereoisomeric effects on mass spectra—I. A review. *Org Mass Spectrom*. 1968;1(5):659-667. doi:10.1002/oms.1210010507

5. Ljungqvist A. Brief history of anti-doping. In: Pitsiladis Y, Rabin O, eds. *Acute Topics in Anti-Doping*. Vol.62. S. Karger AG; 2017. 0

6. World Anti-Doping Agency. 2021 Anti-doping testing figures. 2021; https://www.wada-ama.org/sites/default/files/2023-01/2021_anti-doping_testing_figures_en.pdf. Accessed 31.01.2023.

7. Buisson C, Brooker L, Goebel C, et al. Summer Olympic sports and female athletes: comparison of anti-doping collections and prohibited substances detected in Australia and New Zealand vs. France. *Front Sports Active Living*. 2023;5:1213735. doi:10.3389/fspor.2023.1213735

8. World Anti-Doping Agency. *Prohibited List*. 2021; https://www.wada-ama.org/sites/default/files/resources/files/2021list_en.pdf. Accessed 14.06.2021.

9. Sobolevsky T, Krotov G, Dikunets M, Nikitina M, Mochalova E, Rodchenkov G. Anti-doping analyses at the Sochi Olympic and Paralympic Games 2014. *Drug Test Anal*. 2014;6(11–12):1087-1101. doi:10.1002/dta.1734

10. World Anti-Doping Agency. WADA technical document – TD2023IDCR. https://www.wada-ama.org/sites/default/files/2023-02/td2023idcrv1.1_eng_final.pdf. Accessed 05.06.2023, 2023.

11. Thevis M, Schänzer W. Mass spectrometry in sports drug testing: structure characterization and analytical assays. *Mass Spectrom Rev*. 2007;26(1):79-107. doi:10.1002/mas.20107

12. Vouros P, Harvey D. Method for selective introduction of trimethylsilyl and perdeuteriotrimethylsilyl groups in hydroxy steroids and its utility in mass spectrometric interpretations. *Anal Chem*. 1973; 45(1):7-12. doi:10.1021/ac60323a017

13. Donike M, Zimmermann J. Zur Darstellung von Trimethylsilyl-, Triethylsilyl- und tert.-Butyldimethylsilyl-enoläthern von Ketosteroiden für gas-chromatographische und massenspektrometrische Untersuchungen. *J Chromatogr A*. 1980; 202(3):483-486. doi:10.1016/s0021-9673(00)91836-3

14. Schänzer W, Donike M. Metabolism of anabolic steroids in man: synthesis and use of reference substances for identification of anabolic steroid metabolites. *Anal Chim Acta*. 1993;275(1):23-48. doi:10.1016/0003-2670(93)80274-O

15. Marcos J, Pozo OJ. Derivatization of steroids in biological samples for GC–MS and LC–MS analyses. *Bioanalysis*. 2015;7(19):2515-2536. doi:10.4155/bio.15.176

16. Makin HLJ, Honour JW, Shackleton CHL, Griffiths WJ. General methods for the extraction, purification, and measurement of steroids by chromatography and mass spectrometry. In: Makin HLJ, Gower DB, eds. *Steroid Analysis*. Springer Netherlands; 2010:163-282.

17. Massé R, Laliberté C, Tremblay L. Gas chromatography—mass spectrometry of epimeric 19-norandrostan-3-ol-17-ones as the trimethylsilyl ether, methyloxime. Trimethylsilyl ether and trimethylsilyl-enol trimethylsilyl ether derivatives. *J Chromatogr B Biomed Sci Appl*. 1985;339:11-23. doi:10.1016/S0378-4347(00)84623-X

18. Xu J, Zhu G, Zhang H, Liu J, Jiang K. Differentiation of isomeric cresols by silylation in combination with gas chromatography/mass spectrometry analysis. *Rapid Commun Mass Spectrom*. 2020;34(3): e8576. doi:10.1002/rcm.8576

19. Fragkaki AG, Angelis YS, Tsantili-Kakoulidou A, Koupparis M, Georgakopoulos C. Statistical analysis of fragmentation patterns of electron ionization mass spectra of enolized-trimethylsilylated anabolic androgenic steroids. *Int J Mass Spectrom*. 2009;285(1):58-69. doi:10.1016/j.ijms.2009.04.008

20. Thevis M, Schänzer W. Mass spectrometric analysis of androstan-17β-ol-3-one and androstadiene-17β-ol-3-one isomers. *J Am Soc Mass Spectrom*. 2005;16:1660-1669. doi:10.1016/j.jasms.2005.06.007

21. Kollmeier AS, de la Torre X, Müller C, Botrè F, Parr MK. In-depth gas chromatography/tandem mass spectrometry fragmentation analysis of formestane and evaluation of mass spectral discrimination of isomeric 3-keto-4-ene hydroxy steroids. *Rapid Commun Mass Spectrom*. 2020;34(24):e8937. doi:10.1002/rcm.8937

22. Kollmeier AS, Parr MK. Mass spectral fragmentation analyses of isotopically labelled hydroxy steroids using gas chromatography/electron ionization low-resolution mass spectrometry: a practical approach. *Rapid Commun Mass Spectrom*. 2020;34(12):e8769. doi:10.1002/rcm.8769

23. Assaf J, Kollmeier AS, Müller C, Parr MK. Reconsidering mass spectrometric fragmentation in electron ionization mass spectrometry – new insights from recent instrumentation and isotopic labelling exemplified by ketoprofen and related compounds. *Rapid Commun Mass Spectrom*. 2019;33(2):215-228. doi:10.1002/rcm.8313

24. McCloskey JA, Stillwell RN, Lawson A. Use of deuterium-labeled trimethylsilyl derivatives in mass spectrometry. *Anal Chem*. 1968; 40(1):233-236. doi:10.1021/ac60257a071

25. Partridge L, Midgley I, Djerassi C. Mass spectrometry in structural and stereochemical problems. 249. Elucidation of the course of the characteristic ring D fragmentation of unsaturated steroids. *J Am Chem Soc*. 1977;99(23):7686-7695.

26. Schänzer W. Metabolism of anabolic androgenic steroids. *Clin Chem*. 1996;42(7):1001-1020. doi:10.1093/clinchem/42.7.1001

27. Loke S, Liu L, Wenzel M, et al. New insights into the metabolism of methyltestosterone and metandienone: detection of novel A-ring reduced metabolites. *Molecules*. 2021;26(5):1354. doi:10.3390/molecules26051354

28. Poole CF. Alkylsilyl derivatives for gas chromatography. *J Chromatogr A*. 2013;1296:2-14. doi:10.1016/j.chroma.2013.01.097

29. Fenselau CC, Robinson CH. Critical distance for functional group interaction on electron impact. *J Am Chem Soc*. 1971;93(12):3070-3071. doi:10.1021/ja00741a055

30. Fragkaki AG, Angelis YS, Koupparis M, Tsantili-Kakoulidou A, Kokotos G, Georgakopoulos C. Structural characteristics of anabolic androgenic steroids contributing to binding to the androgen receptor and to their anabolic and androgenic activities: applied modifications in the steroidal structure. *Steroids*. 2009;74(2):172-197. doi:10.1016/j.steroids.2008.10.016

31. Harvey DJ, Vouros P. Mass spectrometric fragmentation of trimethylsilyl and related alkylsilyl derivatives. *Mass Spectrom Rev*. 2020;39(1–2):105-211. doi:10.1002/mas.21590

32. Parr MK, Zapp J, Becker M, Opfermann G, Bartz U, Schänzer W. Steroidal isomers with uniform mass spectra of their per-TMS derivatives: synthesis of 17-hydroxyandrostan-3-ones, androst-1-, and −4-ene-3,17-diols. *Steroids*. 2007;72(6):545-551. doi:10.1016/j.steroids.2007.03.006

33. Parr MK, Opfermann G, Geyer H, et al. Seized designer supplement named "1-androsterone": identification as 3β-hydroxy-5α-androst-1-en-17-one and its urinary elimination. *Steroids*. 2011;76(6):540-547. doi:10.1016/j.steroids.2011.02.001

34. Dumaswala R, Setchell KD, Zimmer-Nechemias L, Iida T, Goto J, Nambara T. Identification of 3 alpha,4 beta,7 alpha-trihydroxy-5 beta-cholanoic acid in human bile: reflection of a new pathway in bile acid metabolism in humans. *J Lipid Res*. 1989;30(6):847-856. doi:10.1016/S0022-2275(20)38314-0

35. Kohler M, Parr MK, Opfermann G, et al. Metabolism of 4-hydroxyandrostenedione and 4-hydroxytestosterone: mass spectrometric identification of urinary metabolites. *Steroids*. 2007; 72(3):278-286. doi:10.1016/j.steroids.2006.11.018

36. Dürbeck HW, Büker I. Studies on anabolic steroids. The mass spectra of 17α-methyl-17β-hydroxy-1,4-androstadien-3-one (dianabol) and its metabolites. *Biomed Mass Spectrom*. 1980;7(10):437-445. doi:10.1002/bms.1200071007

37. Borges CR, Taccogno J, Crouch DJ, Le L, Truong TN. Structure and mechanism of formation of an important ion in doping control. *Int J Mass Spectrom*. 2005;247(1):48-54. doi:10.1016/j.ijms.2005.08.013

38. Egger H, Spiteller G. Massenspektren und Stereochemie von Hydroxyverbindungen, 1. Mitt.: Hydroxysteroide. *Monatsh Chem Verw Teile Anderer Wiss*. 1966;97(2):579-601. doi:10.1007/BF00905276

SUPPORTING INFORMATION

Additional supporting information can be found online in the Supporting Information section at the end of this article.